ISSN 1674-1056
http://cpb.iphy.ac.cn
http://iopscience.iop.org/cpb
中国物理 B
Chinese Physics
中国物理
Chinese Physics B

The effect of replacing pnictogen elements on the physical properties of $SrMg_2X_2$ (*X*=N, P, As, Sb, Bi) Zintl compounds

G Murtaza, Abdul Ahad Khan, M Yaseen, A Laref, Naeem Ullah, Inayat ur Rahman
Citation: Chin. Phys. B . 2018, 27(4): 047102. **doi:** 10.1088/1674-1056/27/4/047102

Journal homepage: http://cpb.iphy.ac.cn; http://iopscience.iop.org/cpb

What follows is a list of articles you may be interested in

Density functional theory analysis of electronic structure and optical properties of La-doped Cd_2SnO_4transparent conducting oxide

Mei Tang(汤梅), Jia-Xiang Shang(尚家香), Yue Zhang(张跃)
Chin. Phys. B . 2018, 27(1): 017101. **doi:** 10.1088/1674-1056/27/1/017101

Topological nodal line semimetals

Chen Fang(方辰), Hongming Weng(翁红明), Xi Dai(戴希), Zhong Fang(方忠)
Chin. Phys. B . 2016, 25(11): 117106. **doi:** 10.1088/1674-1056/25/11/117106

Observation of trapped light induced by Dwarf Dirac-cone in out-of-plane condition for photonic crystals

Subir Majumder, Tushar Biswas, Shaymal K Bhadra
Chin. Phys. B . 2016, 25(10): 107102. **doi:** 10.1088/1674-1056/25/10/107102

First-principles calculations of structural and electronic properties of $Tl_xGa_{1-x}As$ alloys

G. Bilgeç Akyüz, A. Y. Tunali, S. E. Gulebaglan, N. B. Yurdasan
Chin. Phys. B . 2016, 25(2): 027101. **doi:** 10.1088/1674-1056/25/2/027101

Theoretical optoelectronic analysis of intermediate-band photovoltaic material based on $ZnY_{1-x}O_x$(*Y*=S, Se, Te) semiconductors by first-principles calculations

Wu Kong-Ping, Gu Shu-Lin, Ye Jian-Dong, Tang Kun, Zhu Shun-Ming, Zhou Meng-Ran, Huang You-Rui, Zhang Rong, Zheng You-Dou
Chin. Phys. B . 2013, 22(10): 107103. **doi:** 10.1088/1674-1056/22/10/107103

The effect of replacing pnictogen elements on the physical properties of $SrMg_2X_2$ (X = N, P, As, Sb, Bi) Zintl compounds*

G Murtaza[1,†], Abdul Ahad Khan[2], M Yaseen[3], A Laref[4], Naeem Ullah[5], and Inayat ur Rahman[1]

[1] *Materials Modelling Labortary, Department of Physics, Islamia College University, Peshawar, Pakistan*

[2] *Department of Physics, University of the Peshawar, KP, Pakistan*

[3] *Department of Physics, University of Agriculture, Faisalabad* 38040, *Pakistan*

[4] *Department of Physics and Astronomy, College of Science, King Saud University, Riyadh* 11451, *King Saudi Arabia*

[5] *Department of Physics, City University of Hong Kong, Hong Kong* 999077, *China*

(Received 13 December 2017; revised manuscript received 17 January 2018; published online 10 March 2018)

The effect of replacing the anion from N to Bi down the group in the periodic table is investigated on $SrMg_2X_2$ (X = N, P, As, Sb, Bi). A full potential linearized augmented plane wave plus local orbitals method is used along with different exchange–correlation potentials to obtain the lattice constants, phonons, electronic, and optical properties of the $SrMg_2X_2$ (X = N, P, As, Sb, Bi) Zintl compounds. A good agreement is achieved and our calculations are validated by previous experimental and theoretical data. All compounds have shown stable dynamical behavior with gamma centered longitudinal response having no imaginary frequencies. Electronic band structures reveal the semiconducting nature of the compounds. The Pnictogen (X)-p state contributed mainly in the valence band and the Sr-d state forms the conduction of the compounds. Relative charge transfer and low overlapping of the atomic densities indicates the preferable ionic bonding character of these materials. In the optical properties, real and imaginary parts of dielectric function, complex refractive index, birefringence, reflectivity, and optical conductivity are calculated. These compounds can be utilized in the optical and optoelectronic devices.

Keywords: Zintl compounds, band structure, optical response

PACS: 71.15.Mb, 73.20.At, 74.25.Gz **DOI:** 10.1088/1674-1056/27/4/047102

1. Introduction

In recent years, nitride materials showed important technological applications.[1] Nitrogen is stable under normal conditions and may react with selected elements with interesting properties to form different compounds.[2] Synthesis and structural characterization of $SrMg_2N_2$ have been reported in Ref. [3] The single crystal of $SrMg_2N_2$ was colorless plates, transparent with a hexagonal shape. To improve the mechanical strength of Mg_3Sb_2, Guodong *et al.*[4] suggested that the weak ionic bond between Mg–Sb should be enhanced by proper doping strategies, for instance partial substitution of magnesium (Mg) via more electropositive cation of strontium (Sr). The $SrMg_2N_2$ compound shows a ductile behavior and a striking elastic anisotropy. It is found that $SrMg_2N_2$ had a direct bandgap (Γ–Γ) and converted to indirect gap (Γ–M) at 5.16 GPa.

Using the quasi-harmonic Debye model, thermal effects on some macroscopic properties of $SrMg_2N_2$ have been studied.[5] The electronic profiles and transport phenomena of Zintl phase $SrMg_2Pn_2$ (Pn = As, Sb, Bi) compounds and Mg_3Sb_2 by the first principles calculations have been reported.[6] The theoretical investigations of transport properties and electronic structures of Zintl compounds $SrMg_2X_2$ X = Sb, Bi) were calculated by using the *ab-initio* method and the semi-classical Boltzmann theory within the constant relaxation time approximation.[7] Novel systems, such as AMg_2B_2 (A = Ca, Sr, Ba; B = As, Sb, Bi) have been arranged and structurally characterized by x-ray single crystal investigations.[8] They crystallize in trigonal phase and isotypic in the ordered anti-La_2O_3(Ce_2O_2S)-type structure. The coordination polyhedra of the element (V)-atoms were compared with those in A_2B and A_5B_3 compounds that belonged to the Zintl phases.

The above discussion induces that II–II_2–V_2 Zintl compounds possess important semiconducting properties while many of them are worthy of study. Cation–anion modification gives the opportunity of improvement in the physical properties of semiconducting materials. To acquire the insight, we have systematically studied the structural, electronic, and optical properties of $SrMg_2X_2$ (X = N, P, As, Sb, Bi). The phonon

*Project supported by a grant from the "Research Center of Female Scientific and Medical Colleges", the Deanship of Scientific Research, King Saud University. Yaseen M is thankful to Higher Education Commission (HEC), Pakistan for funding (Grant No. 6410/Punjab/NRPU/R&D/HEC/2016), and also this study is made possible by the support of the United States Government and the American people through the United States Agency for International Development (USAID). The contents are the sole responsibility of National University of Sciences and Technology and do not necessarily reflect the views of USAID or the United States Government.

†Corresponding author. E-mail: murtaza@icp.edu.pk

© 2018 Chinese Physical Society and IOP Publishing Ltd

dispersion calculations carried out promise the dynamic stability of these systems. Stable configuration and optoelectronic properties are of great technological significance of the understudy compounds by performing the augmented plane-wave total energy calculations.

2. Computational details

The full-potential linearized augmented plane wave (FP-LAPW) plus local orbitals (LO)[9] method realized in the Wien2k code[10] was applied to determine the physical properties of the $SrMg_2X_2$ compounds. The Perdew–Burke–Ernzerhof (PBE)[11] and Tran–Blaha modified Becke–Johnson (TB-mBJ)[12] functionals were applied to treating exchange–correlation effects. The plane wave cutoff was set to 500 eV in order to relax both the atomic positions and lattice constants. The crystal structure atomic positions of the elements were relaxed until the energy and forces converged to 10^{-4} eV and 10^{-3} eV/Å, respectively. For the Brillouin zone integration, 1000 k-points were used. The sphere radii of the Sr, Mg, N, P, As, Sb, and Bi were 2.5, 2.4, 2.0, 2.36, 2.5, 2.5, and 2.5, respectively. Dynamical stability was inspected through the phonon dispersion calculations in the quantum espresso package.[13–15] In this method, the dynamical matrix is evaluated at a predetermined reference coarse grid in the wave-vector space through the density functional perturbation theory.[13–15] Employing the Fourier transform of the calculated dynamical matrix at the coarse wave-vector grid, the interatomic force constants are extracted on the corresponding real-space grid to evaluate the frequencies at corresponding symmetry points in the irreducible Brillouin zone.

3. Results and discussion

3.1. Structural and dynamical properties

$SrMg_2X_2$ has a trigonal structure with space group $P\bar{3}m1$ (#164), and with a symmetry of $a = b \neq c$, $\alpha = \beta = 9$, and $\gamma = 12°$. Wyckoff position $1b$ is for Sr and $2d$ position for both Mg and X (N, P, As, Sb, and Bi). The lattice parameters a (in unit Å), c (Å), c/a ratio, bulk modulus B (GPa), pressure derivative (B), ground state volume, and energy are obtained by unit cell volume optimization of $SrMg_2X_2$ compounds. The specimen crystal structure is shown in Fig. 1, while the ground state structural optimization (E–V) curves of all understudy compounds are shown in Fig. 2. The minimum of these parabolic curves corresponds to the lowest ground state energy at the optimum volumes of the unit cell.[16] The calculated ground state structural parameters (lattice constant, bulk modulus, volume, energy) are summarized in Table 1 along with the previous experimental and theoretical data for comparison. The results of our calculations are in agreement with those validated by the previous experimental and theoretical data. As a general trend, the lattice constants (a (Å) and c (Å)) increase as those move down in the periodic table for insertion of anion from N to Bi. Bulk modulus B (GPa) decreases as one move from as we move down the group-V, showing the more compressibility trend and lowering in the hardness of these materials.

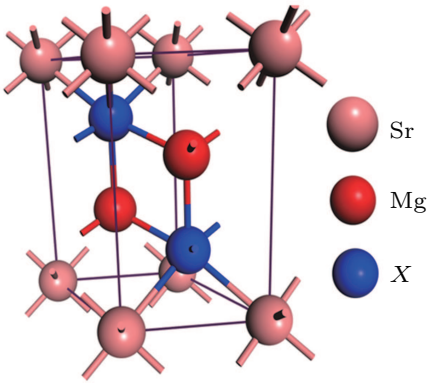


Fig. 1. (color online) Crystal structure specimen of $SrMg_2X_2$ (X = N, P, As, Sb, and Bi) systems.

Table 1. The lattice parameters a, c, c/a ratio, the bulk modulus B, optimum volume (V_0), and ground state total energy (E_0).

Compound	a/Å	c/Å	c/a	V_0/a.u.^{3}	B/GPa	E_0/Ry
$SrMg_2N_2$	3.65 3.622,[3] 3.624,[3] 3.6292[5]	6.362 6.359,[3] 6.346,[3] 6.3421[5]	1.74	496.57	94.80	–7380.33
$SrMg_2P_2$	4.37	7.240	1.65	809.08	53.03	-8529.75
$SrMg_2As_2$	4.43 4.41[6]	7.456 7.41[6]	1.68 1.68[8]	859.39	48.65	–16205.76
$SrMg_2Sb_2$	4.74 4.70[6]	7.879 7.83[6]	1.66 1.66[8]	1037.64	40.23	–33095.85
$SrMg_2Bi_2$	4.81 4.79[6]	8.146 7.93[6]	1.69 1.66[8]	1102.32	34.71	–93487.30

Refs. [3] and [8]: experimental results; Refs. [5] and [6]: theoretical results.

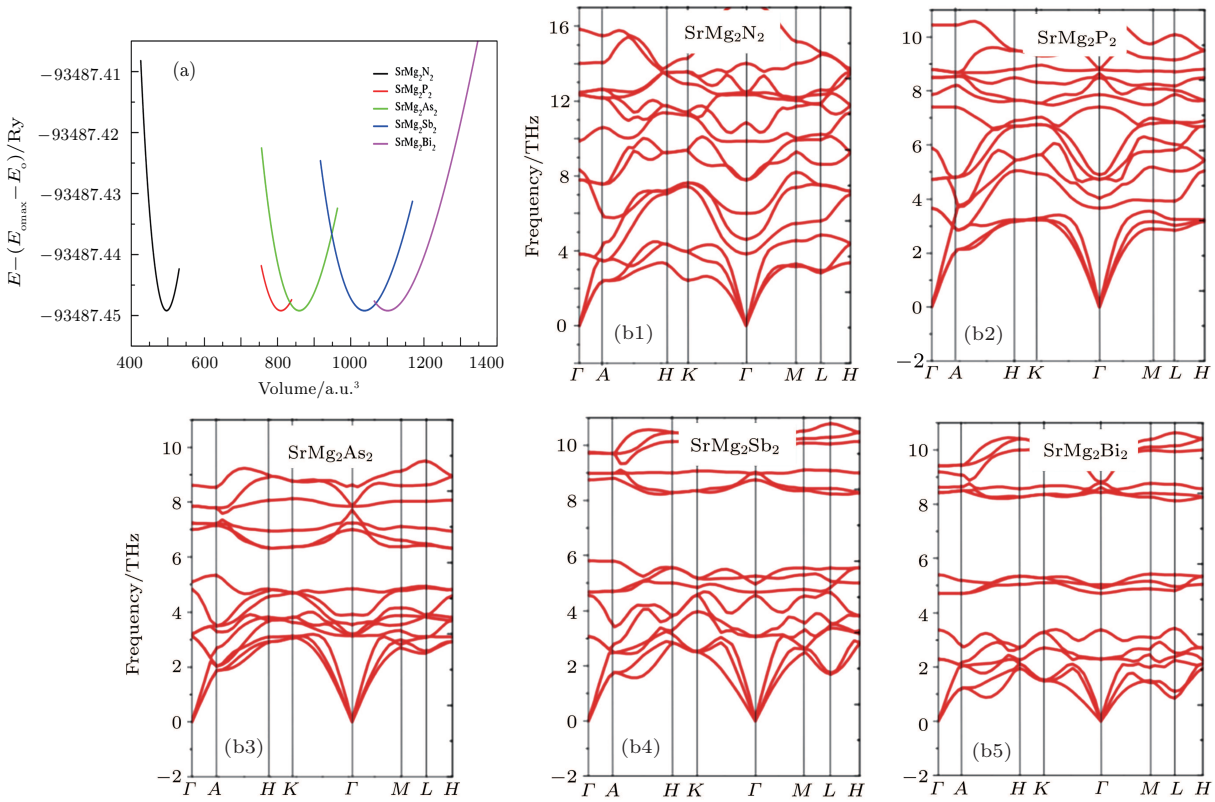


Fig. 2. (color online) (a) Volume optimization (E–V) curves for $SrMg_2X_2$ compounds. E_{omax} is the ground state of the $SrMg_2Bi_2$, while the equation of states of other compounds is also represented here by subtracting the ground state energy (E_0) of the compounds from the ground state energy of $SrMg_2Bi_2$. (b) Phonon dispersions of $SrMg_2X_2$ compounds.

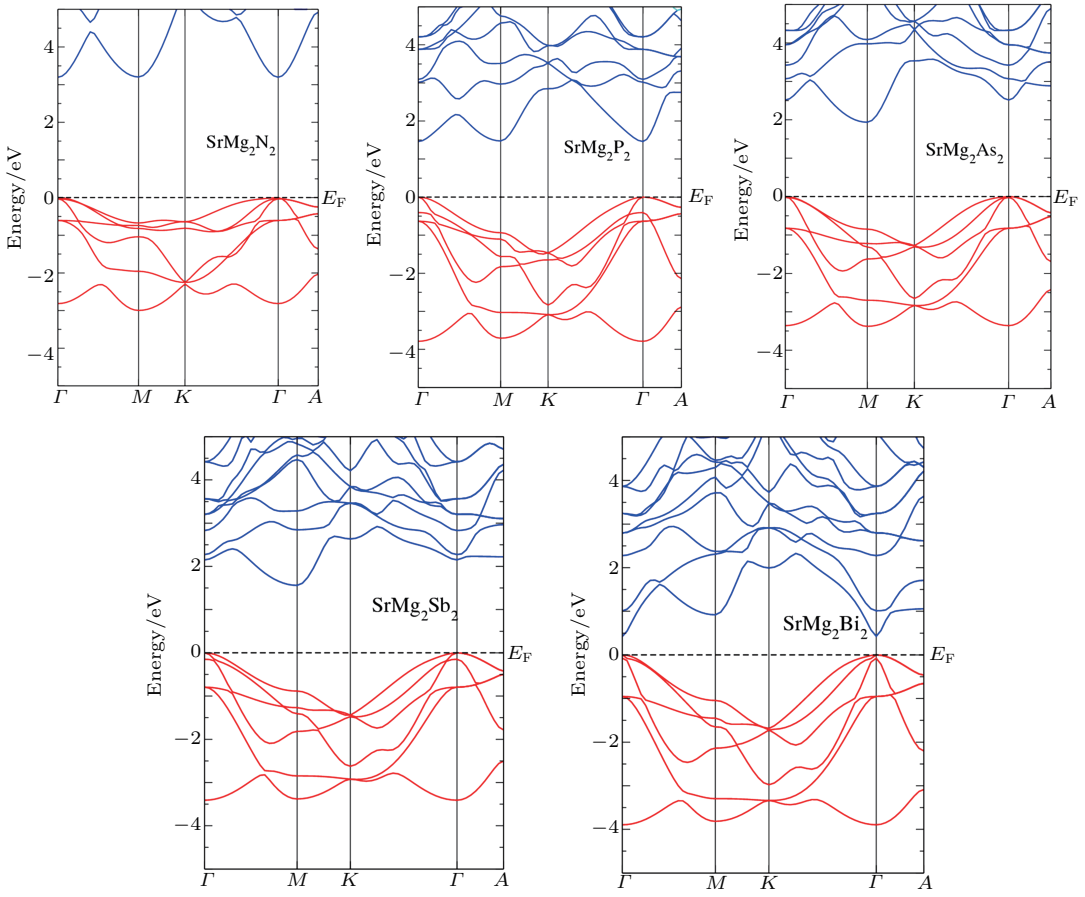


Fig. 3. (color online) Calculated band gap energy using TB-mBJ for $SrMg_2X_2$ (X = N, P, As, Sb, and Bi) compounds.

Variations in the structural parameters with insertion of group-V light to heavy elements probe the electronic and optical properties that in turn depend on the vibrational behavior. A real frequency vibrational response guarantees the dynamical stability of the materials. Therefore, the phonon dispersion calculations are important to investigate the dynamics under the electronic and optical processes. Calculated phonon dispersions are shown in Fig. 3. All compounds have shown stable dynamical behavior with gamma centered longitudinal response having no imaginary frequencies. The general trend of a decrease in the frequencies of the optical modes can be understood as the heavier anion insertion reduces the bulk modulus and elasticity of these compounds. The general trend of the hard to soft optical phonon frequencies also shows the gradual weakening of the bonding while going down the group-V. No imaginary frequencies in all understudied systems confirm the dynamical stability of these materials.

3.2. Electronic properties

Owing to the ground state stable configurations, band structures of $SrMg_2X_2$, (X = N, P, As, Sb, Bi) are calculated using state of the art TB-mBJ exchange–correlation functional. The conduction band minima (CBM) of $SrMg_2X_2$ (X = As, Sb) lies at the M symmetry point and valence band maxima (VBM) lies at the Γ symmetry point, therefore both compounds are indirect band gap along the $\Gamma \rightarrow M$ direction, while the direct band gap of $SrMg_2X_2$ (X = Bi, N, and P) lies at the Γ symmetry point. Our calculation is still in good agreement with the recent published work.[5–7] In all the cases, N-containing cases yielded the highest band gap up to 3.20 eV at a given pnictogen group. The band gap decreases as the pnictogen anions goes down the periodic table from N to P (1.27 eV), then increases for As up to 1.93 eV, again decreasing for Sb up to 1.56 eV, and a sharp decrease in a band gap value up to 0.42 eV for Bi.

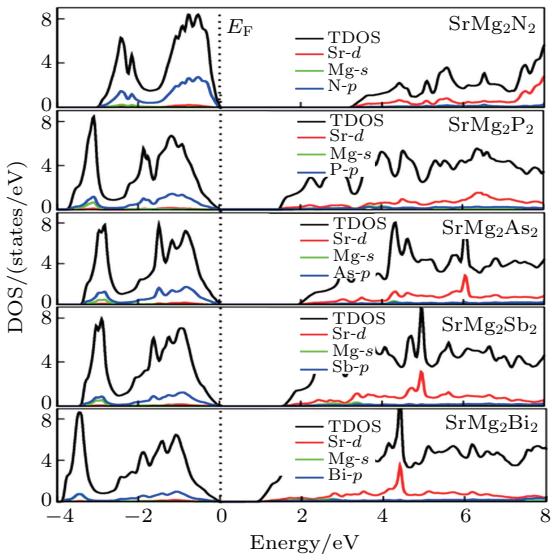


Fig. 4. (color online) Calculated TDOS and PDOS for $SrMg_2X_2$ (X = N, P, As, Sb, and Bi) compounds.

Total density of states (TDOS) and partial density of states (PDOS) plots of $SrMg_2X_2$ compounds are shown in Fig. 4. TB-mBJ functional calculations of the TDOS as well as PDOS are employed to find out the contribution of the electronic states to charge carriers near the Fermi level. In our calculations, we set the Fermi level to the maximum of the valence band and the states with high contribution are plotted for clarity. Contribution to the valence band occupied states is dominated by the anion p-state, while the cation (Sr) s-state has very little and suppressed contribution. The minimum of the conduction band is contributed mainly by the cation (Sr) d-state. The cation–anion contribution of states to the valence and conduction band follows the same pattern for all of these ionic systems. Hence, the exciton structure of these systems will be mainly constituted by a combination of the anion p-state holes carriers and electrons carriers in the d-state of cation (Sr).

3.3. Chemical bonding

The unit cell charge difference density distributions are calculated for investigation of the charge transfer and bonding nature in these systems. The iso-surface of electronic difference charge densities are shown in Fig. 5. It is clear from the figure that strontium has the least iso-surface out of the three elements system showing the least part in bonding of the unit cell. Large donor electron density indicated that magnesium-donated electrons eventually were transferred to the anions having the abundance (red color) of the electronic charge. Relative charge transfer and low overlapping of the atomic densities indicate the preferable ionic bonding character of these materials. Charge transfer can also be understood in terms of the electronegativity difference where group-II elements donates the electrons, while group-V

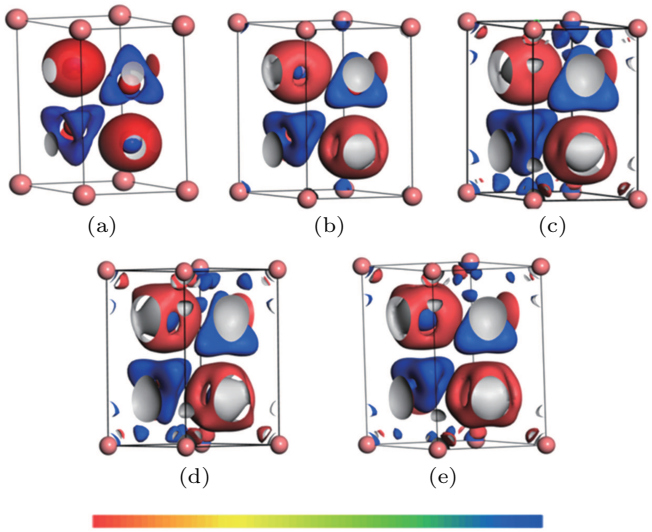


Fig. 5. (color online) Difference charge density iso-surface display of (a) $SrMg_2N_2$, (b) $SrMg_2P_2$, (c) $SrMg_2As_2$, (d) $SrMg_2Sb_2$, and (e) $SrMg_2Bi_2$ unit cells. Red and blue colors indicate the charge abundance and deficiency, respectively, as shown in the color strip.

elements (X = N, P, As, Sb, Bi) are accepter due to their electronegative nature. Furthermore, we have summarized the Mullikan charge distribution in Table 2 to understand the quantitative charge transfer and hence the explanation of the iso-surafce and bonding character. More electronegativity of the group-V decreases down the group as less charge accumulation can be noted while going down the group. Magnesium has the high charge donor value with positive valence charge while significant charge transfer is witnessed from strontium by the Mullikan charge analysis.

Table 2. Mullikan total valence charge and band gap energy of present calculations. Previous theoretical and experimental data on energy gap are also tabulated for comparison.

Compound $SrMg_2X_2$ (X = N, P, As, Sb, and Bi)	Mullikan charge Sr (Mg) X	Band gap energy/eV	Experimental	Theoretical
$SrMg_2N_2$	0.65 (1.00)$^{-1.32}$	3.20	–	1.72[5]
$SrMg_2P_2$	0.87 (0.70)$^{-1.13}$	1.27	–	–
$SrMg_2As_2$	0.88 (0.59)$^{-1.03}$	1.93	–	1.84[6]
$SrMg_2Sb_2$	0.80 (0.54)$^{-0.90}$	1.56	–	1.26[6,7]
$SrMg_2Bi_2$	0.86 (0.37)$^{-0.80}$	0.42	–	0.72[6,7]

Refs. [5], [6], [7]

3.4. Optical properties

$SrMg_2X_2$ (X = N, P, Bi) are direct band gap materials, and these materials might be promising solar cell absorbents. To investigate the possibility, we have calculated the important optical properties like complex dielectric function, reflectivity, complex refractive index, reflectivity and optical conductivity of the understudied materials, and the results are shown in Figs. 6 and 7. The figures show the average optical spectra and not the diagonal components. The anisotropy of the crystals is observed through the birefringence, which is shown in Fig. 8.

The real and imaginary parts are given in Fig. 6(a) and 6(b), which identify the optical dielectric response function for $SrMg_2X_2$ compounds in the energy range of 0 eV to 10 eV. Also, the maximum values for real and imaginary parts of the dielectric function are determined. It is clearly seen from the figures that the static dielectric function $\varepsilon_1(0)$ increases from $SrMg_2N_2$ to $SrMg_2Bi_2$ as expected, while the energy band gap decreases. This inverse feature could be associated with Penn's model.[17] For $SrMg_2N_2$, the sharp peak of $\varepsilon_1(\omega)$ noted to be 7.08 at energy 3.85 eV. Similarly, for $SrMg_2P_2$ the sharp peak of $\varepsilon_1(\omega)$ noted to be 12.38 at energy 3.11 eV. In the same way, $\varepsilon_1(\omega)$ for $SrMg_2As_2$, $SrMg_2Sb_2$, and $SrMg_2Bi_2$ compounds are noted to be 13.71, 16.97, and 20.98 at energy points 3.03, 2.68, and 2.08 eV, respectively. Except $SrMg_2N_2$, whose energy values lie in the ultraviolet spectrum, all the other four compounds have peaks in the visible region of a spectrum. In Fig. 6(b), we display the imaginary part of the optical dielectric function as a function of energy $\varepsilon_2(\omega)$, which is the sum of total ground state transitions from the occupied states of the VB to the unoccupied states CB. This spectrum starts from the fundamental transition edge, which is the excitation of electron from the maximum of valence band to the minimum of the conduction band exhibiting the agreement with the band gap of the materials. This fundamental transition is called the threshold point beyond which the curve increases sharply due to the large interband transitions. Large interband transition incorporates more electrons as the energy of the incident photons increase and hence more optical absorption. Being a narrow band gap material, $SrMg_2Bi_2$ showed large absorption covering the entire visible region together with the near ultraviolet photons. Hence the stable and UV-Vis absorbent $SrMg_2Bi_2$ is a potential candidate for solar cell technology. The $SrMg_2N_2$ has a wide gap (3.20 eV), which cannot accumulate the visible spectrum and show absorption in the ultraviolet region. On the other hand, $SrMg_2P_2$ is a medium gap material showing the absorption in part of the visible region and extending to the ultraviolet photons. Collectively, the family of semiconductors $SrMg_2X_2$ (X = N, P, As, Sb, and Bi) are potential candidates for the solar cells accumulating the visible to ultraviolet energy spectrum. The maximum absorption peaks in the spectra are situated at 5.98, 12.54, 12.59, 16.45, and 22.60 for 8.28, 4.83, 5.31, 4.14, and 2.73 eV for $SrMg_2X_2$, respectively.

Reflectivity of a compound provides information to the surface of the material. In Fig. 7, non-zero components of the optical reflectivity coefficient $R(\omega)$ values are 0.12, 0.19, 0.20, 0.23, and 0.32 for $SrMg_2N_2$, $SrMg_2P_2$, $SrMg_2As_2$, $SrMg_2Sb_2$, and $SrMg_2Bi_2$, respectively, which correspond to reflection at 0 eV. After the limit of zero frequency, reflectivity coefficient $R(\omega)$ enhances with increasing incident photon frequency. Reflectivity maximum arises from the inter band transitions. The figure indicates the prominent reflectance of $SrMg_2X_2$ (X = N, P, As, Sb, Bi). For $SrMg_2N_2$, the maximum reflectivity is noted to be 0.33 at 9.23 eV. Similarly, for $SrMg_2P_2$, $SrMg_2As_2$, $SrMg_2Sb_2$, and $SrMg_2Bi_2$, the maximum reflectivity was found to be 0.54, 0.56, 0.59, and 0.64 at energy 6.95, 6.81, 5.45, and 5.64 eV, respectively.

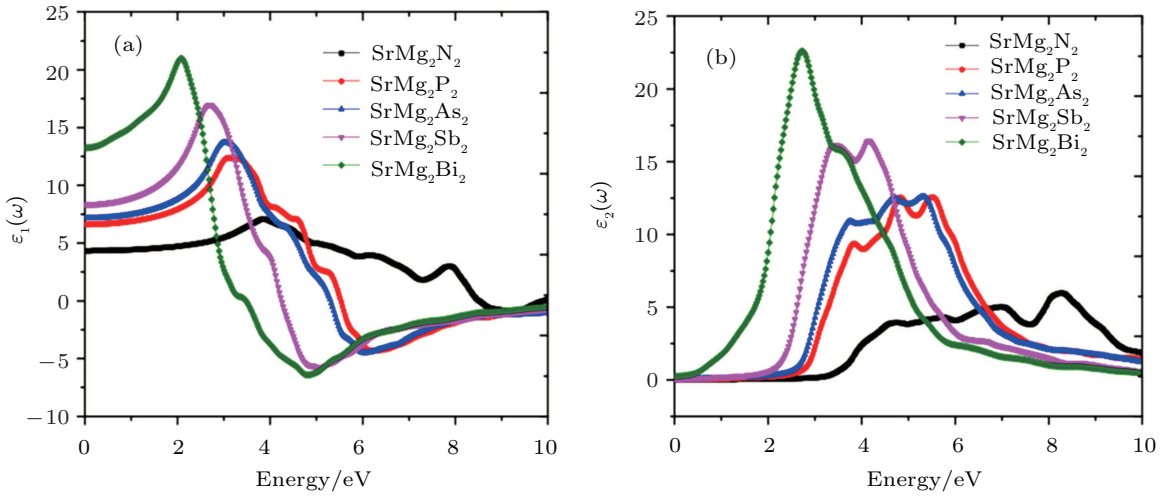


Fig. 6. (color online) (a) Real $\varepsilon_1(\omega)$ and (b) imaginary $\varepsilon_2(\omega)$ parts of the dielectric functions for $SrMg_2X_2$, (X = N, P, As, Sb, and Bi) compounds.

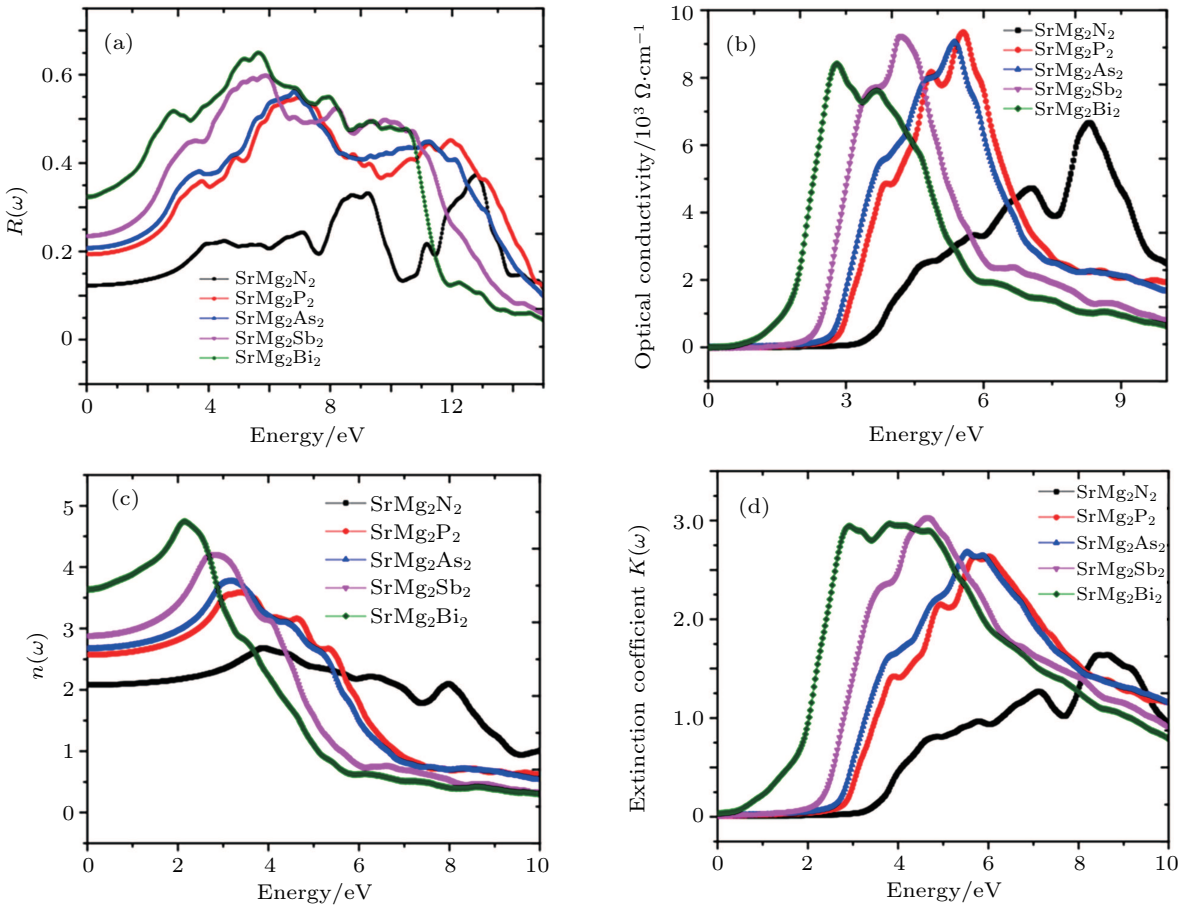


Fig. 7. (color online) Calculated (a) reflectivity spectra, (b) optical conductivity spectra, (c) refractive index, and (d) extinction coefficient versus incident photon energy of $SrMg_2X_2$, (X = N, P, As, Sb, and Bi)

The optical conductivity spectrum $\delta(\omega)$ is shown in Fig. 7(b). The photoconductivity is an optical phenomenon in which electrical conductivity of a material increases due to the absorption of electromagnetic radiation. This spectrum represents the conduction of electrons when applying electromagnetic field. It refers to the conductivity of a material which is created by electron transportation due to photon radiation. The maximum value of $\delta(\omega)$ is found to be 6669, 8162, 9055, 9235, and 8412 Ω^{-1}·cm^{-1} around 8.3, 4.8, 5.3, 4.2, and 2.8 eV for $SrMg_2N_2$, $SrMg_2P_2$, $SrMg_2As_2$, $SrMg_2Sb_2$, and $SrMg_2Bi_2$, respectively. Investigations of this quantity help us to offer new optoelectronic applications for electro-optical devices.

The static refractive index $n(0)$ is obtained in Fig. 7(c), and these results are found to be 2.08, 2.57, 2.67, 2.88, and 3.63 for $SrMg_2N_2$, $SrMg_2P_2$, $SrMg_2As_2$, $SrMg_2Sb_2$, and

$SrMg_2Bi_2$, respectively. These results show that $n(0)$ increases as we move from $SrMg_2N_2$ to $SrMg_2Bi_2$. The imaginary part of the refractive index or extinction coefficient $K(\omega)$ spectrum as a function of the incident photons shows the absorption behavior and closely follows the interband transition of $\varepsilon_2(\omega)$ spectra. The local maxima of $K(\omega)$ corresponding to the zero values of $\varepsilon_1(\omega)$ as shown in Fig. 6(b), are found to be 1.63 at 8.44 eV for $SrMg_2N_2$, 2.63 at 6.02 eV for $SrMg_2P_2$, 2.67 at 5.53 eV for $SrMg_2As_2$, 3.03 at 4.66 eV for $SrMg_2Sb_2$, and 2.96 at 3.82 eV for $SrMg_2Bi_2$, respectively. The $K(\omega)$, as plotted in Fig. 7(d) has a similar trend to $\varepsilon_2(\omega)$, which indicates absorption of the incident electromagnetic energy.

The birefringence is the difference between the extraordinary and ordinary refraction indices, $\Delta n = n_e - n_o$, where n_e is the index of refraction for an electric field oriented along the c axis and n_o is the index of refraction for an electric field perpendicular to the c axis. Figure 8 shows the spectral behavior of the birefringence $\Delta n(\omega)$ for $SrMg_2X_2$ compounds. The presence of birefringence is actually in the nonabsorbing region, which is below the energy gap and contributing to the nonlinear optical behavior. The $\Delta n(\omega)$ spectral dependence shows strong oscillations around zero in the energy range up to 10 eV.

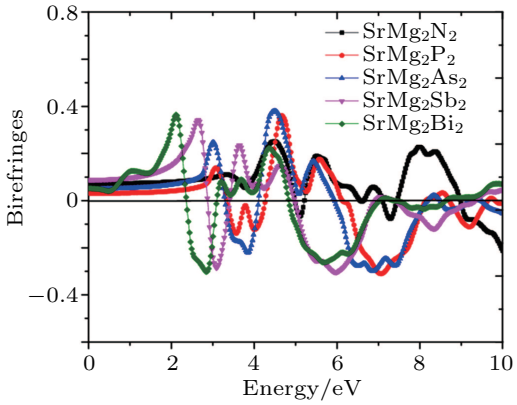


Fig. 8. (color online) Calculated birefringence for $SrMg_2X_2$, (X = N, P, As, Sb, and Bi).

4. Conclusions

The FP-LAPW + LO method along with different exchange–correlation potentials is used to obtain the lattice constants, phonon, electronic and optical properties of the $SrMg_2X_2$ (X = N, P, As, Sb, Bi) Zintl compounds. An inverse relation of the lattice constants and bulk modulus was observed in these compounds by replacement of the cations X from N to Bi. All compounds have shown stable dynamical behavior with gamma centered longitudinal response having no imaginary frequencies. Electronic band structures revealed that $SrMg_2X_2$ (X = As, Sb) are indirect bandgap semiconductors while $SrMg_2X_2$ (X = Bi, N, and P) are direct bandgap. The energy gap decreases by replacing the X anion from N to Bi except for $SrMg_2P_2$. The Pnictogen (X)-p state contributes majorly in the valence band and the Sr-d state mainly forms the conduction band of the compounds. Relative charge transfer and low overlapping of the atomic densities indicate the preferable ionic bonding character of these materials. The real part of the dielectric function, refractive index, and reflectivity static values varies inversely to the energy bandgap. Further, the optical structures are red shifted by replacement of the anions X from N to Bi. All the compounds show strong optical response in the visible and ultraviolet regions of the electromagnetic spectrum. Our study suggested that the proper anion replacements probe the electronic structure and optical absorption profile and might be promising materials in electronics and photovoltaics.

References

[1] Orhan E, Jobic S, Brec R, Marchand R and Saillard J Y 2002 *J. Mater. Chem.* **12** 2475
[2] Prots Y, Niewa R, Schnelle W and Kniep R 2002 *Z. Anorg. Allg. Chem.* **628** 1590
[3] Reckeweg O and DiSalvo F 2001 *Z. Anorg. Allg. Chem.* **627** 371
[4] Li G, Aydemir U, Wood M, An Q, Goddard W A, Zhai P, Zhang Q and Snyder G J 2017 *J. Mater. Chem. A* **5** 9050
[5] Haddadi K, Bouhemadou A and Bin-Omran S 2012 *Comput. Mater. Sci.* **53** 204
[6] Singh D J and Parker D 2013 *J. Appl. Phys.* **114** 143703
[7] Sun J and Singh D J 2017 *J. Mater. Chem. A* **5** 8499
[8] Deller K and Eisenmann B 1977 *Z. Naturforsch. B Chem. Sci.* **32** 612
[9] Andersen O K 1975 *Phys. Rev. B* **42** 3060
[10] Blaha P, Schwarz K, Madsen G K H, Kvasnicka D and Luitz J 2001 *WIEN2k, an Augmented Plane Wave Plus Local Orbitals Program for Calculating Crystal Properties*, Vienna University of Technology, Austria
[11] Perdew J P, Burke K and Ernzerhof M 1996 *Phys. Rev. Lett.* **77** 3865
[12] Tran F and Blaha P 2009 *Phys. Rev. Lett.* **102** 226401
[13] Baroni S, de Gironcoli, Corso S D and Giannozzi P 2001 *Rev. Mod. Phys.* **73** 515
[14] Gonze X and Lee C 1997 *Phys. Rev. B* **55** 10355
[15] Giannozzi P, Baroni S, Bonini N, Calandra M, Car R, *et al.* 2009 *J. Phys.: Condens. Matter* **21** 395502
[16] Seddik T, Uğur G, Khenata R, Uğur S, Soyalp F, Murtaza G, Rai D P, Bouhemadou A and Omran S B 2016 *Chin. Phys. B* **25** 107801
[17] Penn D R 1962 *Phys. Rev.* **128** 2093